Supporting Information

Photogranulation in a Hydrostatic Environment Occurs with Limitation of Iron

Abeera A. Ansari [†,‡], Arfa A. Ansari [†], Ahmed S. Abouhend [†], Joseph G. Gikonyo [†] and Chul Park [†*]

[†] Department of Civil and Environmental Engineering, University of Massachusetts, Amherst, MA 01002, USA

[‡] U.S.-Pakistan Center for Advanced Studies in Energy (USPCAS-E), National University of Sciences & Technology (NUST), H-12 Sector (44000), Islamabad, Pakistan

*corresponding author: chulp@umass.edu

Summary

Number of pages: 13 (S1-S13)

Number of Tables: 2

Number of Figures: 7

Detailed Materials and Methods

Bulk liquid filtration for Fe. Fe in bulk liquid passing through Ultracel 30 kDa ultra-filtration membrane (EMD Millipore Corporation, Billerica, MA, USA) was considered as dissolved Fe.[32] Bulk liquid was also passed through 0.45 μm mixed cellulose ester membrane (Fisher Scientific, USA). Fe in the size fraction smaller than 0.45 μm and greater than 30 kDa was considered colloidal Fe.

Estimation of phycobilin concentration in photogranular biomass. Ten mL mixed biomass sample was centrifuged at 12000 rpm for 10 min. After discarding the supernatant, the pellet was re-suspended in 0.025 M phosphate buffer saline solution (pH 7.2). The sample was then subjected to homogenization at 700 rpm for 1 min (IKA T18 basic Ultra-Turrax), followed by sonication (Fisher Scientific Sonic Dismembrator Model 500) at 20% strength for 2 min. After centrifugation, the obtained supernatant was filtered through 0.22 μm syringe filter (Basix, Fisher Scientific) and its absorbance was read at 566 nm, 620 nm, 652 nm, and 750 nm using a portable spectrometer (DR 2700, Hach, US). Absorbance λ_{max} for phycoerythrin, phycocyanin and allophycocyanin was obtained at 566 nm, 620 nm, and 652 nm, respectively, by using phycobilin standards (Prozyme, US). Absorbance at 750 nm represented the background interference, which was subtracted from other wavelengths.[39] Corrected 566 nm, 620 nm, and 652 nm absorbances were introduced in the Bennett and Bogorad equations[37] to quantify the concentrations of respective phycobilin.

Extraction of extracellular polymeric substances (EPS) from photogranular biomass. A twenty mL biomass sample was centrifuged at 12000 rpm for 10 min at 4 °C. The resulting supernatant was replaced by 10 mL phosphate buffer solution (10 mM NaCl, 1.2 mM KH_2PO_4, and 6 mM Na_2HPO_4), after which the sample was proceeded to homogenization at 700 rpm for

30 s (IKA T18 basic Ultra-Turrax) and sonication (Fisher Scientific Sonic Dismembrator Model 500) at 10% strength for 40 s. The sample was centrifuged, and the resulting supernatant was filtered through 0.45 μm cellulose filter to obtain EPS extract by sonication. The remaining pellet was subjected to base treatment by re-suspending it in 10 mL phosphate buffer solution and bringing its pH to 10.5-11 using 1 M NaOH.[33] The sample was then shaken at 425 rpm for 2 h at 4 °C and centrifuged. The supernatant was filtered through 0.45 μm cellulose filter to get the EPS extract by base treatment.[33]

Table S1. Pearson correlation between phycobilin and other photosynthetic pigments produced during cultivations.

	Phycobilin		
	Amherst	Hadley	Springfield
Chlorophyll a	0.94	0.79	0.70
Chlorophyll b	0.64	0.63	0.70
Chlorophyll c	0.51	0.27	0.66

Table S2. Pearson correlation between Fe and organic matter in bulk liquid.

		Amherst		Hadley		Springfield	
		Colloidal Fe	Dissolved Fe	Colloidal Fe	Dissolved Fe	Colloidal Fe	Dissolved Fe
		30 kDa<Fe< 0.45μm	Fe <30 Kda	30 kDa<Fe< 0.45μm	Fe <30 Kda	30 kDa<Fe< 0.45μm	Fe <30 Kda
Dissolved organic nitrogen (DON)	Colloidal bulk liquid fraction	**-0.86**	-0.62	-0.31	-0.01	0.06	0.14
	Dissolved bulk liquid fraction	0.29	0.06	0.07	-0.32	-0.18	-0.50
Dissolved organic carbon (DOC)	Colloidal bulk liquid fraction	-0.58	-0.23	-0.04	0.13	0.10	0.13
	Dissolved bulk liquid fraction	-0.46	-0.51	-0.29	-0.55	-0.54	**-0.76**

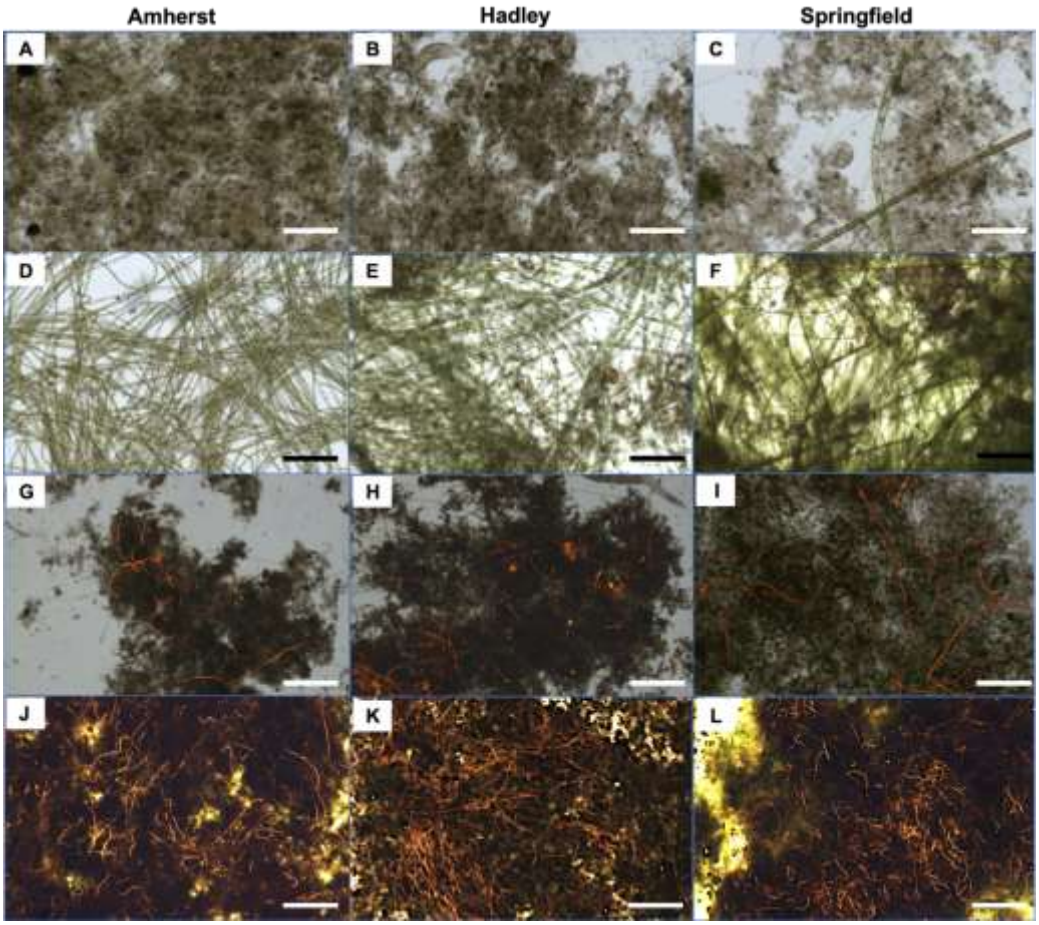

Figure S1. Microscopy of samples during hydrostatic cultivation of photogranules. Panels A-C (on day 5, brightfield microscopy) show the growth of unicellular and filamentous green algae in the top layer of settled sludge biomass. Panels D-F (between day 9-12, brightfield microscopy) display outgrowth of filamentous green algae. Panels G-I (between day 9-12, autofluorescence microscopy) illustrate the appearance of cyanobacteria (indicated by golden-orange fluorescence) in top layer of settled biomass. Panels J-L (between day 15-18, autofluorescence microscopy) shows the growth of filamentous cyanobacteria which eventually dominated the phototrophic community. Scale bars for panels A-F and I are 400 μm; scale bars for panels G-H and J-L are 2000 μm.

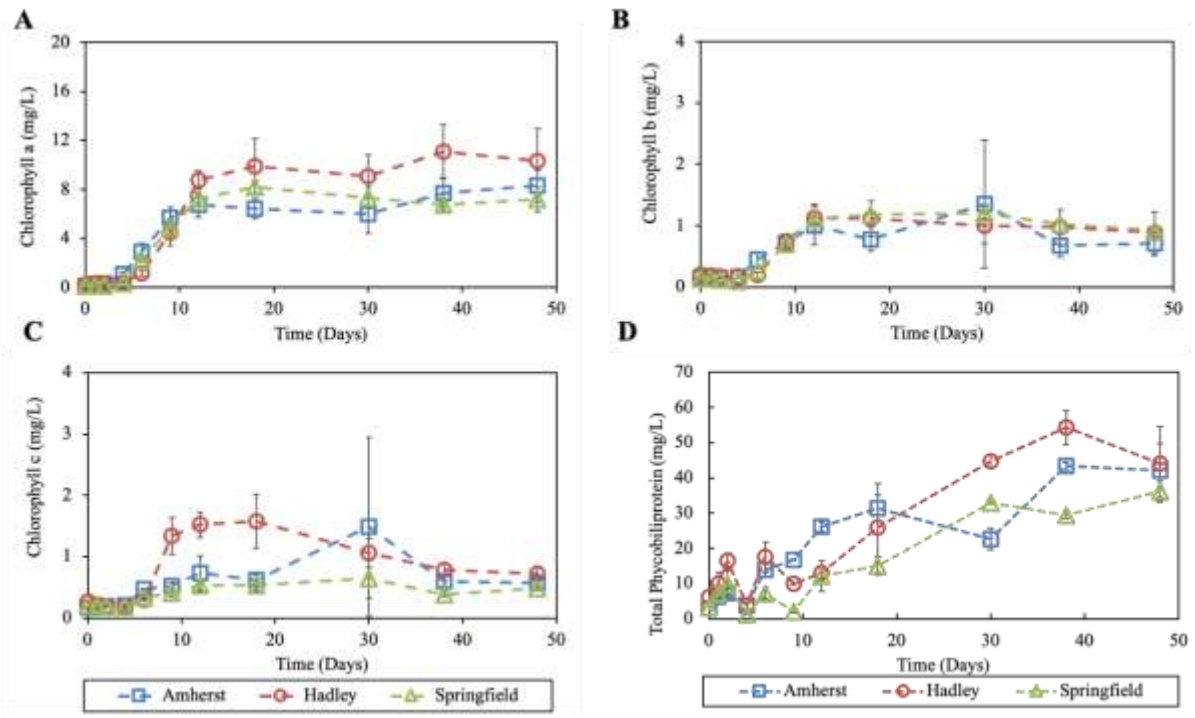

96

97 **Figure S2.** Changes in photopigment concentrations during the progression of
98 photogranulation under hydrostatic conditions using three different activated sludges as
99 inoculum. (A) chlorophyll a, (B) chlorophyll b, (C) chlorophyll c, and (D) total
100 phycobiliprotein. Error bars represent standard deviation from triplicate samples.

101

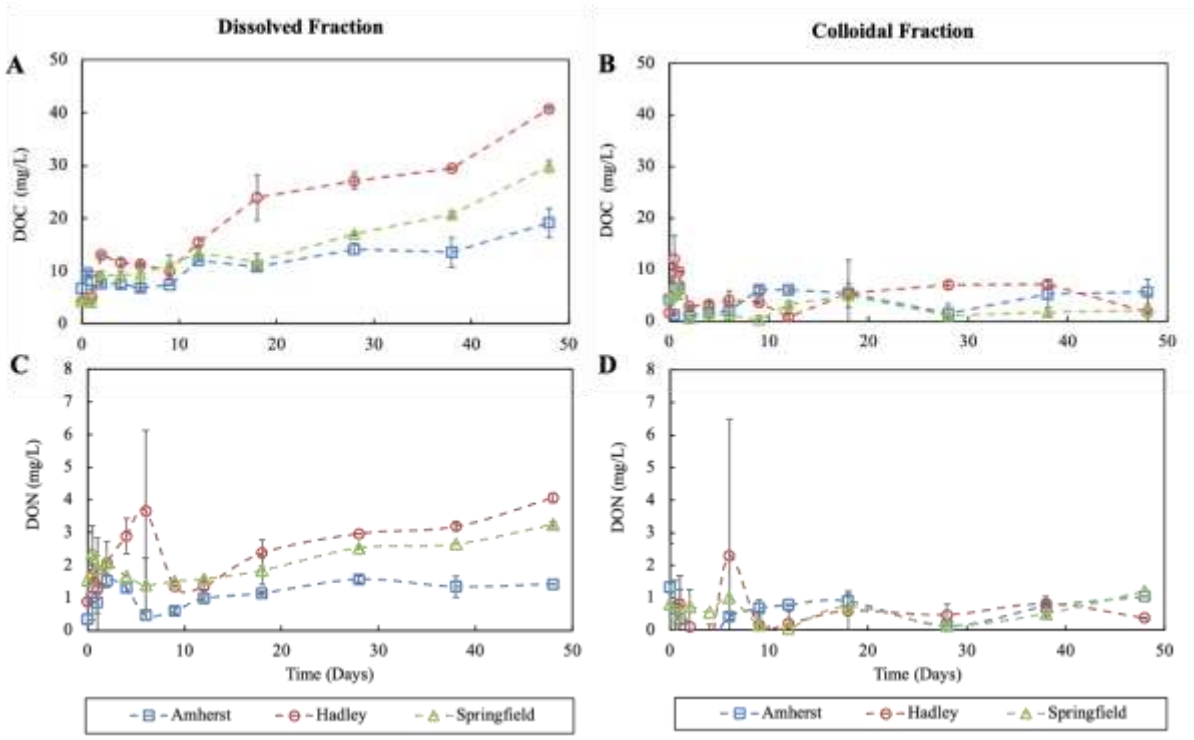

Figure S3. Changes in dissolved organic carbon (DOC) (A, B) and dissolved organic nitrogen (DON) (C, D) in the fractions of dissolved bulk liquid (<30 kDa) and colloidal bulk liquid (0.45μm – 30 kDa) during the progression of photogranulation under hydrostatic conditions. Error bars represent the range of results from duplicate samples.

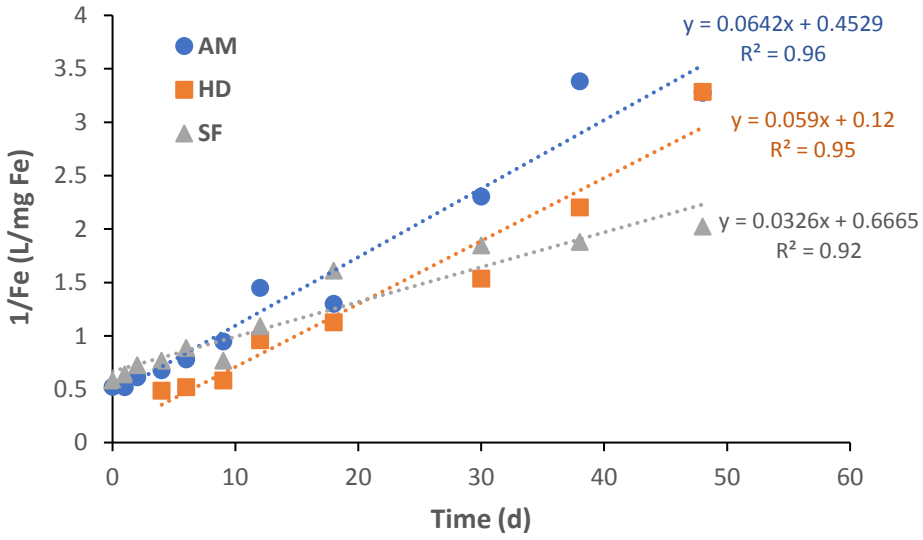

Figure S4. Curve fitting analysis showing second-order reaction of Fe_{EPS} in hydrostatic cultivation.

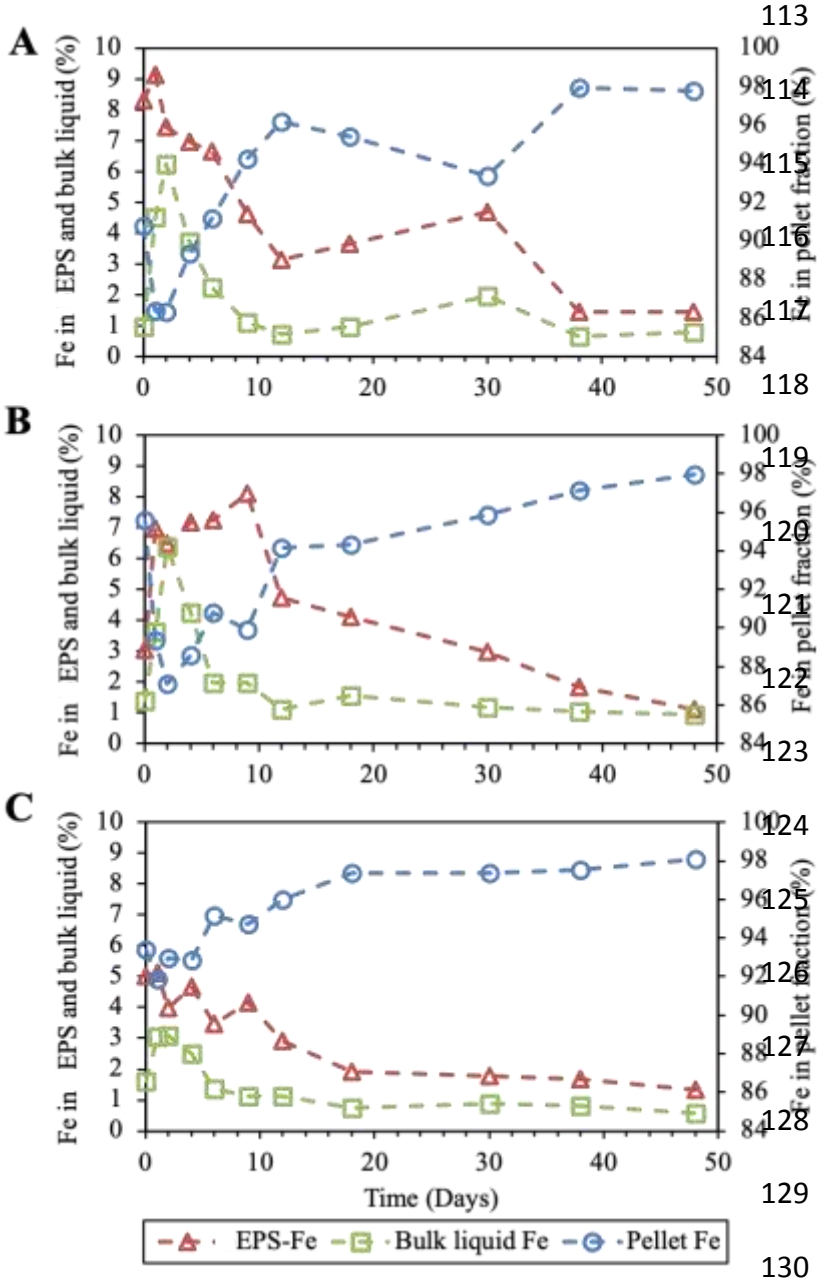

Figure S5. Distribution of Fe (%) in different fractions of biomass during the photogranulation process in a hydrostatic environment. Activated sludge inoculums: (A) Amherst, (B) Hadley, and (C) Springfield activated sludges.

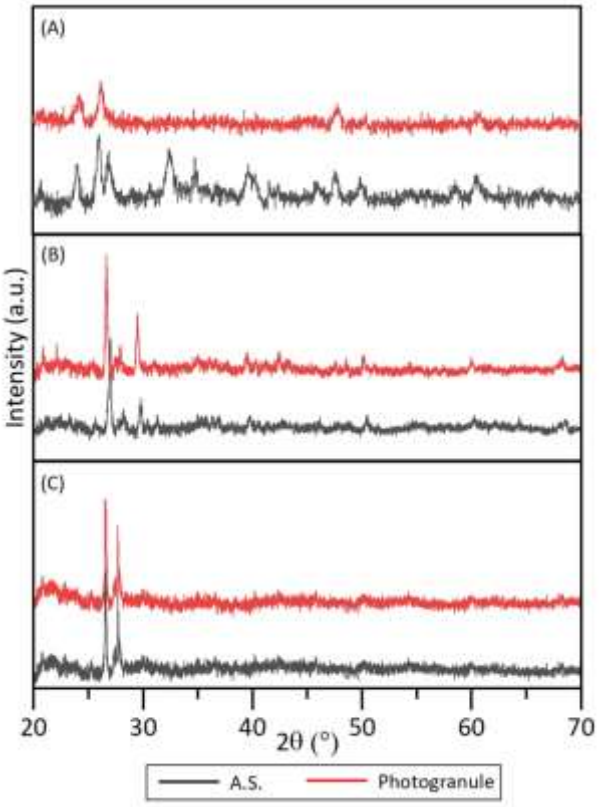

Figure S6. Powder X-Ray diffraction patterns of activated sludge (A.S.) and OPG (photogranule) in hydrostatic cultivations of (A) Amherst, (B) Hadley, and (C) Springfield sets. The results show the existence of iron mostly in amorphous forms. We did not observe a complete diffraction pattern for any known crystalline ferric oxide. Furthermore, many oxides have overlapping diffraction patterns which made PXRD analysis complicated.

FTIR analysis of vacuumed-dried biomass.

Figure S7 depicts the FTIR spectra of activated sludge and OPG biomass. The typical O−H broad stretching peak centered at 3300 cm^{-1} (Peak 1) suggests the formation of ferric oxyhydroxide Fe(O)OH and/or ferric hydroxides $Fe(OH)_3$ in both activated sludge and OPG samples. The progression of OPG occurred, after initial anaerobic conditions, in oxic (Figure 4) and circumneutral pH (6.5-8) environment, which is known to favor the formation of insoluble ferric hydroxides. Swanner *et al.*[53] stated that cyanobacterium *Synechococcus* PCC 7002 oxidized Fe (II) to ferric oxyhydroxide via chemical oxidation using photosynthetic oxygenation. The O-H group stretches can also potentially belong to the carboxylic group of polysaccharides (PS). These FTIR results along with earlier correlation analysis between bEPS-PS and Fe might indicate possible complexation between Fe (III) and PS. The interactions between proteins (PN) and Fe (III) were also depicted in FTIR spectra. Peaks related to PN were found at 1637-1640 cm^{-1} (Peak 2), 1531-1541 $cm^{-}1$ (Peak 3) and 1225-1233 cm^{-1} (Peak 4), which corresponded to amide C=O carbonyl group, amide II (N−H) double bond, and C−O stretching bond of COOH, respectively.[56,57] These peaks decreased in intensity during the photogranulation process. The decline in these functional groups seems to support the decrease in EPS-PN, which was also strongly correlated with Fe_{EPS} in this study. Apart from EPS-PN, FTIR spectra also displayed the relative increase in C-O stretching bond of PS (1024-1066 cm^{-1}, Peak 5) in Hadley. Earlier studies showed that cyanobacteria accumulate Fe precipitates on their outer polysaccharide sheath.[54,55] The increasing EPS-PS content could, therefore, possibly contain Fe either as insoluble Fe (III) precipitate (accumulation via adsorption) or Fe complexation with carbonyl/carboxylic groups.

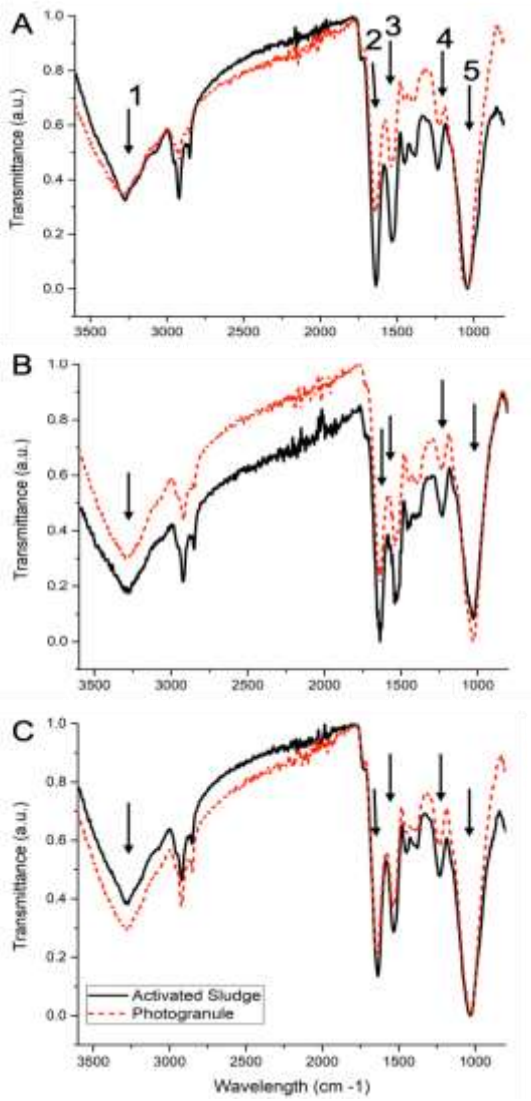

178

179 **Figure S7.** Room-temperature FTIR spectra of activated sludge (A.S.) and OPG
180 (photogranule) in hydrostatic cultivations of (A) Amherst, (B) Hadley, and (C) Springfield sets.
181 Peak 1 (centered at 3300 cm^{-1}) shows O-H bond stretching, Peak 2 (1637–1640 cm^{-1}) shows
182 amide C=H carbonyl group band, Peak 3 (1531–1541cm^{-1}) shows N-H (2nd-amide) double
183 bond, Peak 4 (1225–1233cm^{-1}) shows C-O stretching band or COOH, and Peak 5 (1024–1066
184 cm^{-1}) belongs to C-O stretching bond.

185